ERDC/CRREL TR-22-1

Cold Regions Research and Engineering Laboratory

US Army Corps of Engineers®
Engineer Research and Development Center

ERDC
ENGINEER RESEARCH & DEVELOPMENT CENTER

Terrain and Signature Physics Integration Center

A Study on the Delta-Bullington Irregular Terrain Radiofrequency Propagation Model

Assessing Model Suitability for Use in Decision Support Tools

Daniel J. Breton

January 2022

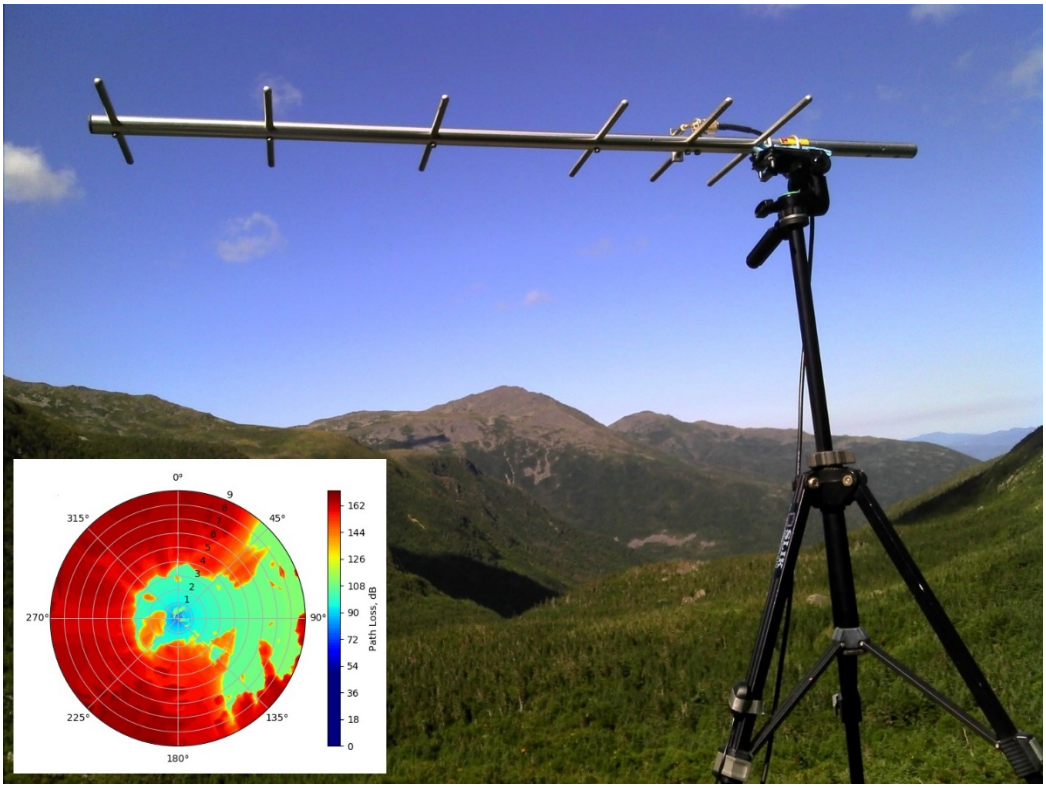

The U.S. Army Engineer Research and Development Center (ERDC) solves the nation's toughest engineering and environmental challenges. ERDC develops innovative solutions in civil and military engineering, geospatial sciences, water resources, and environmental sciences for the Army, the Department of Defense, civilian agencies, and our nation's public good. Find out more at www.erdc.usace.army.mil.

To search for other technical reports published by ERDC, visit the ERDC online library at https://erdclibrary.on.worldcat.org/discovery.

ERDC/CRREL TR-22-1
January 2022

A Study on the Delta-Bullington Irregular Terrain Radiofrequency Propagation Model

Assessing Model Suitability for Use in Decision Support Tools

Daniel J. Breton

U.S. Army Engineer Research and Development Center (ERDC)
Cold Regions Research and Engineering Laboratory (CRREL)
72 Lyme Road
Hanover, NH 03755-1290

Final Report

Prepared for U.S. Army Engineer Research and Development Center
3909 Halls Ferry Road
Vicksburg, MS 39180-6199

Under ERDC Future Innovation Fund, FAD/Customer Order 4902-XX-2460-08,
"Terrain and Signature Physics Integration Center"

Abstract

Modeling the propagation of radiofrequency signals over irregular terrain is both challenging and critically important in numerous Army applications. One application of particular importance is the performance and radio connectivity of sensors deployed in scenarios where the terrain and the environment significantly impact signal propagation. This report investigates both the performance of and the algorithms and assumptions underlying the Delta-Bullington irregular terrain radiofrequency propagation model discussed in International Telecommunications Union Recommendation P.526-15. The aim is to determine its suitability for use within sensor-planning decision support tools. After reviewing free-space, spherical earth diffraction, and terrain obstacle diffraction losses, the report discusses several important tests of the model, including reciprocity and geographic continuity of propagation loss over large areas of rugged terrain. Overall, the Delta-Bullington model performed well, providing reasonably rapid and geographically continuous propagation loss estimates with computational demands appropriate for operational use.

Contents

Figures and Tables

Figures

Tables

Preface

This study was conducted for U.S. Army Engineer Research and Development Center (ERDC) under the ERDC Future Innovation Fund, FAD/Customer Order 4902-XX-2460-08, "Terrain and Signature Physics Integration Center."

The work was performed by the Signature Physics Branch of the Research and Engineering Division, ERDC Cold Regions Research and Engineering Laboratory (CRREL). At the time of publication, Dr. Steven Peckham was branch chief, Dr. George W. Calfas was division chief, and Dr. Robert E. Davis was the technical director for Geospatial Research and Engineering. The deputy director of ERDC-CRREL was Mr. David B. Ringelberg, and the director was Dr. Joseph L. Corriveau.

COL Teresa A. Schlosser was commander of ERDC, and Dr. David W. Pittman was the director.

1 Introduction

1.1 Background

Modeling the propagation of radiofrequency (RF) waves over irregular terrain has been the subject of research for roughly 80 years (Bullington 1947; Kasampalis et al. 2015). Such work, originally developed to ensure adequate separation of broadcast towers to avoid co-channel interference and support frequency reuse, has expanded to include analysis of radar range and ground-clutter contributions (Ayasli 1986; Lin and Reilly 1997); prediction of the performance of mobile communications systems (Neskovic, Neskovic, and Paunovic 2000); and, of course, planning the layout of cellular telephone networks (Lee 1985).

Other aspects of RF propagation modeling of direct importance to the Army include determining optimal placement of RF-sensing devices and estimating the performance of networked communications between sensors, particularly those deployed in complex terrain. The Environmental Awareness for Sensor and Emitter Employment (EASEE) decision support tool software developed at the U.S. Army Engineer Research and Development Center's Cold Regions Research and Engineering Laboratory (ERDC-CRREL) enables realistic, physics-based modeling and simulation of signal emission, propagation, and sensing for a number of different modalities (Wilson, Bates, and Yamamoto 2008; Wilson and Yamamoto 2014). The goal of EASEE is to provide timely and operationally relevant guidance on optimal sensor placement and sensor performance to military and homeland security operators in the field, where computational resources may be limited.

EASEE has utilized external, commercially produced RF propagation software (Yamamoto, Reznicek, and Wilson 2015) in the past, but this placed significant constraints on the ability to distribute the software and incurred significant computational overhead to correctly georeference and spatially interpolate the propagation losses predicted by the external software. To fully realize capabilities for the RF domain and to avoid issues associated with an external propagation model, it is necessary to fully integrate a propagation loss model capable of accounting for irregular terrain and over-the-horizon conditions into EASEE itself. This report documents

the underlying algorithms and overall performance of a RF propagation loss model suitable for implementation within EASEE.

1.2 Overview of terrestrial radiofrequency propagation models

Tropospheric RF propagation models can be roughly divided into two groups: those that explicitly account for the terrain over which the signal must propagate and those that ignore the specifics of the terrain. The former are often called "site-specific" or "terrain-integrated" models, of which the Integrated Terrain Model (ITM; Hufford, Longley, and Kissick 1982) and Terrain Integrated Rough Earth Model (TIREM; Powell 1983) are examples. The latter "non-site-specific" models generally depend on only distance and some very general characterization of the propagation terrain and are typically used in cases where the terrain is too complex or only order-of-magnitude results are required. The Okumura-Hata urban propagation model (Okumura et al. 1968) is an example of such a non-site-specific model.

Primary challenges to site-specific modeling include

- the necessary simplification of the propagation terrain to make the problem tractable;
- evaluation of multiple diffracting obstacles and approximately summing their losses; and
- correctly combining multiple, sometimes competing, loss mechanisms in different regions of the propagation path.

Significant effort has gone into developing various approaches to address these challenges (Bullington 1977; Deygout 1966; Egli 1957; Giovaneli 1984; Lebherz, Wiesbeck, and Krank 1992; Vogler 1982; Yang et al. 1998; Powell 1983), and it is from these numerous approaches that I chose an appropriate method to use within EASEE.

1.3 Objectives

EASEE must rapidly supply believable, physics-based RF predictions using limited computational resources and input data. Therefore, the goal of this work was to find and test a radio propagation model that is straightforward to implement in computer code, suitable for the needs of a tactical user in terms of input data and processing speed, and compatible with the data structures already present within EASEE.

Given these constraints and having reviewed numerous other open-source models for RF propagation, I decided upon the Delta-Bullington method (described in International Telecommunications Union Recommendations P.452-16 [ITU 2015] and P.526-15 [ITU 2019]) as an algorithm that strikes a reasonable balance between fidelity and computational expense when compared against other methods (Bibb et al. 2014). Further, it is reasonably well documented, and proper operation of the EASEE implementation can be tested against a comprehensive set of test propagation paths and verification values for intermediate and final values of the path loss computation.

The Delta-Bullington method includes three major loss mechanisms: free-space or direct transmission losses, diffraction losses over the (smooth) spherical surface of the earth, and diffraction losses from obstacles. This report discuss each of these losses in the following sections, documenting the main techniques and important assumptions contained within this method.

1.4 Approach

Many other open-source RF propagation models exist with widely varying levels of accuracy, technical rigor, computational cost, and quality of documentation. I therefore took a two-stage approach to this study to evaluate the model from both technical and completeness-of-documentation standpoints.

The first stage was to verify that the ITU diffraction model as documented in ITU (2015, 2019) was comprehensible and mathematically consistent. After satisfactorily completing the first stage, the second stage was to actually implement (in the Python programming language) and test the model for both the ITU-provided point-to-point test cases and for the more comprehensive, multiazimuth use cases typically required for propagation mapping by EASEE. Sections 2 through 5 of this report summarize my efforts in the first stage, while sections 6 and 7 describe the results found in the second stage.

2 Free Space or Direct Transmission

Free-space or direct transmission losses account for only the geometrical spreading of radio power density over the surface of a sphere. When combined with the expression for effective antenna aperture, one obtains (assuming matched impedance and polarization) the Friis equation (Friis 1946) for received power

$$P_r = \frac{P_t G_t G_r \lambda^2}{(4\pi)^2 r^2},$$

where

P_t = the transmit power,
G_t = the transmitter antenna gains,
G_r = the receiver antenna gains,
λ = the wavelength, and
r = the separation distance between transmitter and receiver.

In practical units, this can be written as

$$P_{r,\mathrm{dBm}} = P_{t,\mathrm{dBm}} + G_{t,\mathrm{dB}} + G_{r,\mathrm{dB}} - 20\log_{10}(r_{\mathrm{km}}) - 20\log_{10}(f_{\mathrm{MHz}}) - 32.44,$$

which is valid with separation distance r expressed in kilometers and frequency f in MHz. The Delta-Bullington method uses this model of propagation loss whenever the receiver has a clear line of sight (LOS) to the transmitter and no objects (including the bulge of the earth) reduce the clearance to less than 60% of the first Fresnel zone, which I discuss next.

3 Smooth-Earth Diffraction

3.1 Fresnel zones

The behavior of diffraction over the surface of the earth relies on understanding the size and clearance of the Fresnel zones over the surface of the earth or of obstacles existing upon the earth's surface. The Fresnel zones are ellipsoids with foci at points *A* (transmitter) and *B* (receiver); the direct ray is along the ellipsoid's major axis. The defining equation is

$$\overline{AM} + \overline{MB} = \overline{AB} + \frac{n\lambda}{2},$$

where

n = an integer 1, 2, 3, ...;
λ = the wavelength; and
M = the set of points on the ellipsoid.

Reflections inside the first (n = 1) Fresnel zone can go from *A* to reflector *M* and thence to *B* with a path length $\lambda/2$ (or less) longer than the direct ray. For a signal reflecting from an object on *M* then, one could expect a maximum phase difference of π radians between direct and reflected rays. Because this phase shift can lead to total or partial cancellation of the direct ray, interactions within the first Fresnel zone are generally quite important for determination of losses along a given path.

Propagation is assumed to be LOS if there is no obstacle anywhere within the first Fresnel zone. Practically speaking, if obstacles are cleared by more than 60% of the first Fresnel zone radius R_1, then diffraction losses are ignored (Levis, Johnson, and Teixeira 2010). The general formula for the *n*th Fresnel zone radius is

$$R_n = \sqrt{\frac{n\,\lambda\,d_1 d_2}{d_1 + d_2}},$$

where d_1 and d_2 are distances along the straight-line path connecting a transmitter and receiver separated by a distance ($d_1 + d_2$). The Fresnel zone radius is a maximum at the midpoint where $d_1 = d_2$. In practical units, the *n*th Fresnel zone radius can also be written as

$$R_{n,\mathrm{m}} = 550\sqrt{\frac{n\, d_{1,\mathrm{km}} d_{2,\mathrm{km}}}{f_{\mathrm{MHz}}\,(d_{1,\mathrm{km}} + d_{2,\mathrm{km}})}},$$

which assumes d_1 and d_2 are in kilometers, f is in megahertz, and yields a radius expressed in meters.

Surfaces with irregularities smaller than 10% of the first Fresnel zone maximum radius can be considered smooth for the purposes of modeling.

3.2 Radio horizon

The distance to the radio horizon depends on antenna height and the radio refraction characteristics of the troposphere. Tropospheric refraction is generally accounted for through use of an "effective" radius for the earth, a_e, which is larger than that of the real earth. Under standard atmospheric conditions, a_e is 4/3 times the actual earth radius, such that a_e is approximately 8500 km (Levis, Johnson, and Teixeira 2010). Variations in atmospheric conditions and weather events can cause the effective radius to change, but these conditions are not included in the model implemented within EASEE.

The distance to the radio horizon for a single antenna at height h_1 above ground level, then, is

$$d_{LOS,1} = \sqrt{2a_e h_1};$$

and the shared radio horizon distance between one antenna at height h_1 and another at height h_2 is

$$d_{LOS} = \sqrt{2a_e}\left(\sqrt{h_1} + \sqrt{h_2}\right).$$

3.3 Smooth-earth diffraction loss

There are two important cases to consider when calculating diffraction losses accrued due to propagation over a smooth earth:

1. The separation between transmitter and receiver exceeds the distance to the shared radio horizon d_{LOS}, otherwise known as "over-the-horizon" propagation.

2. The separation between transmitter and receiver is less than the shared radio horizon, but the earth's bulge reduces the clearance of the first Fresnel zone to less than 60%.

The smooth-earth diffraction loss method outlined in ITU Recommendation P.526-15 uses a simple interpolation procedure to smoothly join these two cases at d_{LOS} (ITU 2019).

3.3.1 Case 1: Over-the-horizon propagation

In the case of over-the-horizon propagation, the diffraction losses in decibels relative to the free-space losses can be expressed as

$$20 \log_{10} \frac{E}{E_0} = F(X) + G(Y_1) + G(Y_2),$$

where

X = the normalized path length between the terminals,
Y_1 and Y_2 = the normalized heights of the terminal antennae, and
E = the field strength relative to the free-space field strength E_0.

The functions F and G empirically account for distance and antenna height gain effects respectively; little physical insight can be gained from the form of these functions, so this report will not review them here.

The normalized path length X is given by

$$X = \beta d \left(\frac{\pi}{\lambda a_e^2} \right)^{1/3},$$

and the normalized antenna height Y_i is given by

$$Y_i = 2\beta h_i \left(\frac{\pi^2}{\lambda^2 a_e} \right)^{1/3},$$

where

d = the path length between the transmitter and receiver,
λ = the wavelength,
a_e = the effective radius of the earth, and

h_i = the antenna heights (i = 1 for transmitter, i = 2 for receiver) above the smooth surface of the earth.

β is a constant, used at all locations within the domain of interest, related to the electrical properties of the earth and the polarization of the propagating wave. For most conceivable use cases of EASEE, β will be equal to 1; the main exception would be for vertically polarized signals lower than 300 MHz over a significant path length of ocean.

For completeness, this report includes the equations defining β for both horizontal and vertical polarizations. For circular polarization, the value of β should lie somewhere between that of the vertical and horizontal values; but as stated above, β will be unity for any polarization, linear or circular, for all practical cases encountered within EASEE.

In the horizontal case, the effective surface admittance of the earth is

$$K_H = \left(\frac{2\pi a_e}{\lambda}\right)^{-1/3} ((\varepsilon_r - 1)^2 + (60\,\lambda\,\sigma)^2)^{-1/4};$$

and in the vertical polarization case, the surface admittance is

$$K_V = K_H(\varepsilon_r{}^2 + (60\,\lambda\,\sigma)^2),$$

where

ε_r = the effective dielectric permittivity of the earth's surface relative to vacuum and
σ = the effective conductivity of the earth's surface in siemens per meter.

The model can then determine β from

$$\beta = \frac{1 + 1.6K^2 + 0.67K^4}{1 + 4.5K^2 + 1.53K^4}.$$

Typical values of *K* are between zero and 1; higher values indicate increasing importance of the electrical characteristics of the ground. If *K* turns out to be greater than 1, probably the approximate formulas above are not good enough, and the numerical code GRWAVE (available from the ITU) should be used to evaluate *K*. However, this is only a concern for vertically

polarized signals with wavelengths greater than 60 m, far from the anticipated use case for any RF propagation models within EASEE.

3.3.2 Case 2: Within-horizon PROPAGATION

Diffraction losses can still occur for terminals within their shared radio horizon if the first Fresnel zone interacts with the bulge of the earth itself. The analysis of this scenario begins by first defining the length of the path over the curved surface of the earth between transmitter and receiver antennae as d (Figure 1).

Figure 1. Sketch of geometry for within-horizon propagation over a smooth, spherical earth of radius a_e.

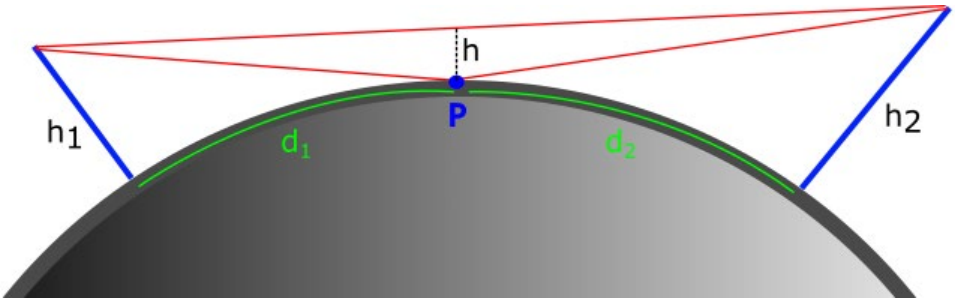

Then the model calculates the smallest clearance height h between the earth and the straight-line path between the terminals, which involves first evaluating three geometrical parameters m, c, and b:

$$m = \frac{d^2}{4a_e(h_1 + h_2)},$$

$$c = \frac{h_1 - h_2}{h_1 + h_2},$$

$$b = \left(\frac{4(m+1)}{3m}\right)^{1/2} \cos\left[\frac{\pi}{3} + \frac{1}{3}\operatorname{acos}\left[\frac{3c}{2}\sqrt{\frac{3m}{(m+1)^3}}\right]\right].$$

From these parameters, the model determines $d_1 = (d/2)(1 + b)$, $d_2 = d - d_1$, and the smallest clearance height

$$h = \frac{d_2\left(h_1 - \frac{d_1^2}{2a_e}\right) + d_1\left(h_2 - \frac{d_2^2}{2a_e}\right)}{d},$$

where d_1 and d_2 are distances from transmitter and receiver, respectively, to the reflection point P at the closest point of approach between the curved earth and the straight-line path between the antennae. This geometry is shown in Figure 1.

Next, the model must determine the required clearance height over the earth bulge such that there are no diffraction losses,

$$h_{req} = 0.552\sqrt{\frac{\lambda\, d_1 d_2}{(d_1 + d_2)}},$$

which is recognizable as a slightly modified form of the first Fresnel zone radius equation. In the case where $h > h_{req}$, there are no diffraction losses; and the loss for this path would be simply calculated as the direct transmission loss defined in an earlier section. However, if $h < h_{req}$, then the model must smoothly account for blockage of the first Fresnel zone as described below.

First, calculate a modified effective earth radius

$$a_{em} = \frac{1}{2}\left[\frac{d}{\sqrt{h_1} + \sqrt{h_2}}\right]^2$$

and then use a_{em} in place of a_e to evaluate the spherical earth diffraction loss parameters X, Y_1, and Y_2 described above in Case 1. The diffraction loss associated with these parameters is designated A_h. If $A_h \leq 0$, then sufficient clearance of the first Fresnel zone exists, and there are no diffraction losses on the path. However, if $A_h > 0$, then the model interpolates to find the final diffraction loss over the entire path as

$$A = A_h\left(1 - \frac{h}{h_{req}}\right),$$

which is expressed in decibels referenced to the free-space loss over the same path length d.

3.3.3 Example calculation

Figure 2 shows an example calculation performed at 3 GHz with both transmit and receive antenna heights at 10 m above the ground.

Figure 2. Propagation losses relative to free-space losses using both Case 1 and Case 2 of the spherical earth diffraction model.

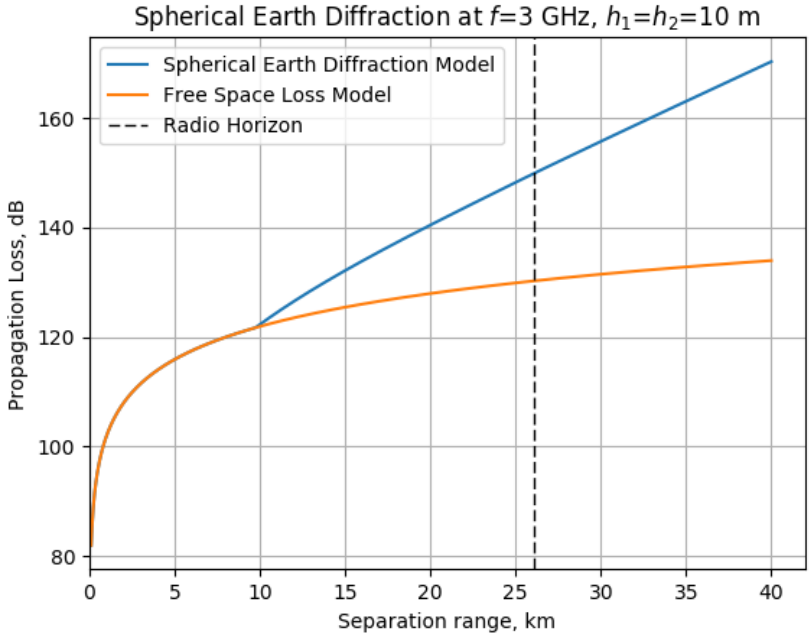

For separation distances less than about 10 km, the antennae enjoy a purely line-of-sight link, and thus the only losses incurred are those associated with direct transmission. Though the shared radio horizon does not occur until 26 km, the impact of within-horizon losses is observable starting at around 10 km where the first Fresnel zone begins to interact with the spherical earth surface. The within-horizon interpolation (Case 2) smoothly matches the over-the-horizon (Case 1) losses, which begin at the radio horizon.

4 Knife-Edge Diffraction

One of the few diffraction geometries that lends itself to a compact, closed-form solution is that of the semi-infinite plane obstacle oriented perpendicular to the direction of incident wave propagation (Durgin 2008). This scenario is generally referred to as "knife-edge" diffraction (KED) and has been substituted for more-complex obstacles in many propagation models, including the Bullington model. The KED geometry can be analyzed in a number of different ways to arrive at a single, unitless parameter v, which is the only argument to the KED loss equation. The definition used in the diffraction models implemented in EASEE is

$$v = h\sqrt{\frac{2}{\lambda}\left(\frac{1}{d_1}+\frac{1}{d_2}\right)},$$

where

h = the height of the top of the obstacle above a straight line connecting the two ends of the path (if the obstacle top is below this line, then $h < 0$) and

d_1 and d_2 = are the distances of the transmitter and the receiver, respectively, from the top of the obstacle.

The exact KED loss, expressed in decibels, is

$$J_{exact}(v) = -20\ \log_{10}\left(\tfrac{1}{2}\sqrt{[1-C(v)-S(v)]^2+\ [C(v)-S(v)]^2}\right),$$

where

$$C(v) = \int_0^v \cos(t^2)\,dt$$

defines the Fresnel cosine integral evaluated at v and

$$S(v) = \int_0^v \sin(t^2)\,dt$$

is the Fresnel sine integral evaluated at v. Plotting this as a function of v in Figure 3, the KED solution shows oscillatory behavior near 0 dB when the

obstacle is well below the direct path and then rapidly increasing diffraction losses as the obstruction height increases.

Figure 3. Knife-edge diffraction, at 440 MHz and $d_1 = d_2 = 100$ m, as a function of obstruction height. (TX = transmitter; RX = receiver.)

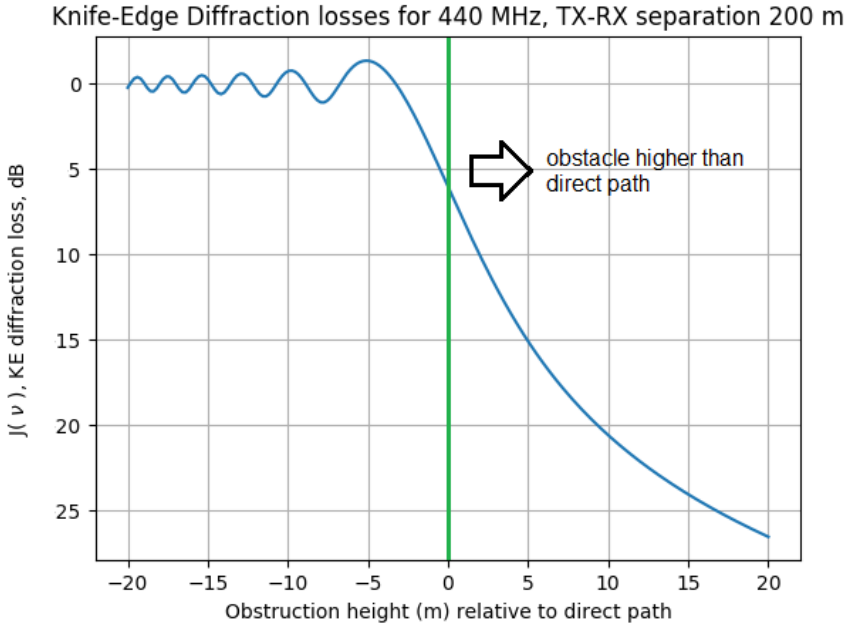

Evaluating the Fresnel integrals can become computationally expensive, and therefore previous studies have developed several approximations. One of the simplest approximations, valid for $\nu > -0.78$, is

$$J(\nu) = 6.9 + 20\log_{10}\left(\sqrt{(\nu - 0.1)^2 + 1} + \nu - 0.1\right),$$

which returns the diffraction loss in decibels and is the approximation used within the EASEE implementation of KED. For $\nu < -0.78$, our implementation simply returns zero, as this is well into the portion of the solution that oscillates rapidly about zero.

5 Bullington Diffraction Model

The Bullington diffraction model (Bullington 1947, 1977) uses a very simple geometric construction (see Figure 4) to determine the visual horizons of both the transmitter and receiver. From these horizons, the model generates a single, effective knife-edge obstruction used to estimate the diffraction losses over the entire path, regardless of the actual number or height of obstructions.

Figure 4. Sketch of the Bullington diffraction model geometry. The transmitter horizon is defined by the obstacle on the far *left*, the receiver horizon is defined by obstacle on the far *right*, and the effective knife-edge obstruction is shown as a *dashed heavy line* near the *center*.

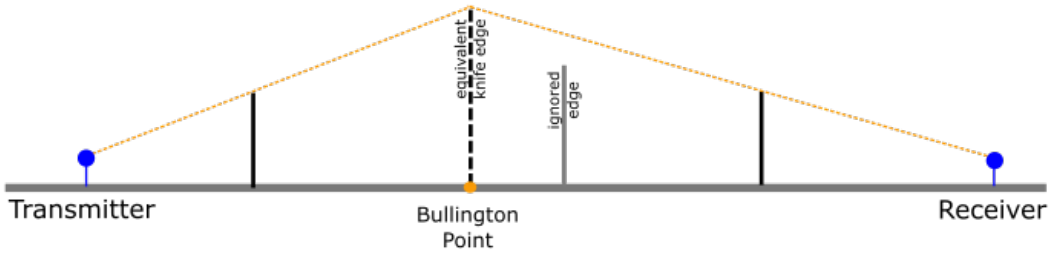

The general premise behind this model is this: the obstacles that define the transmitter and receiver horizons are those that should have the greatest impact on the diffraction losses over the path. In practice, because the Bullington model ignores all but the horizon-defining obstructions, it generally underestimates the losses over a given path (Giovaneli 1984; Pogorzelski 1982). Nevertheless, this report presents details of the Bullington model as it is used (twice) within the Delta-Bullington model described in the next section.

5.1 Elevation definitions and profiles

A primary input to the Bullington method is the elevation profile of terrain lying in a vertical plane containing both the transmitter and receiver antennae, similar to both ITM (Hufford, Longley, and Kissick 1982) and TIREM (Eppink and Kuebler 1994). However, unlike ITM and TIREM, this elevation profile *need not have uniform spacing* of elevation points within the profile.

The elevation profile for the Bullington method must therefore be defined by *two* arrays: $d_{i=1..n}$ stores the distance (in kilometers) along the propaga-

tion path, and $h_{i=1..n}$ stores elevations above mean sea level (m ASL), corresponding to the appropriate distances $d_{i=1..n}$. The elevations of the ground (m ASL) underneath the transmitter h_{gt} and receiver h_{gr} are stored in h_1 and h_n, respectively. The heights of the transmitting and receiving antennae in meters above ground level (m AGL) are h_{tg} and h_{rg}, respectively. The transmit and receive antenna heights (m ASL) are defined as $h_{ts} = h_{gt} + h_{tg} = h_1 + h_{tg}$ and $h_{rs} = h_{gr} + h_{rg} = h_n + h_r$, respectively. These definitions are seemingly tedious but become important later on when the Delta-Bullington method mixes Bullington and spherical earth diffraction elevation parameters. ITU Recommendations P.526-15 and P.452-16 must be studied together to clearly understand the definitions and nomenclature used (ITU 2019, 2015).

5.2 Bullington Step 1: Is the path LOS or transhorizon?

The transmitter visual horizon is defined simply as the point on the entire elevation profile that has the greatest slope relative to the ground at the transmit point,

$$S_{tm} = \max_{i=2..(n-1)} \left[\frac{h_i - h_{ts} + 500 C_e d_i (d_p - d_i)}{d_i} \right].$$

Here $C_e = 1/a_e$ is the effective curvature of the earth in inverse kilometers (1/km), the total path length in kilometers is defined as $d_p = \Sigma_{i=1..n} (d_i - d_{i-1})$, and the slope is expressed in meters per kilometer. The last term in the numerator calculates the elevations of the "bulge" of a smooth earth along the propagation path (Levis, Johnson, and Teixeira 2010).

Evaluating the slope of the straight-line path between transmitter and receiver,

$$S_{tr} = \frac{h_{rs} - h_{ts}}{d_p},$$

the model simply compares these slopes to determine if the path is LOS or transhorizon: if $S_{tm} < S_{tr}$, then the path is LOS, and the algorithm proceeds to Step 2a; if $S_{tm} \geq S_{tr}$, then the path is transhorizon, and the algorithm proceeds to Step 2b.

5.3 Bullington Step 2a: Evaluate Fresnel zone losses for LOS case

For the LOS case, it is important to account for profile points that interact with the first Fresnel zone, and this is done by finding the profile point with the maximum KED parameter,

$$\nu_{max} = \max_{i=2\ldots(n-1)} \left\{ \left[h_i + 500 C_e d_i (d_p - d_i) - \frac{h_{ts}(d_p - d_i) + h_{rs} d_i}{d_p} \right] \left(\frac{0.002 d_p}{\lambda d_i (d_p - d_i)} \right)^{1/2} \right\}.$$

The model then determines an *uncorrected* diffraction loss $L_{uc} = J(\nu_{max})$ in decibels using the approximate KED formula and then proceeds to Step 3.

5.4 Bullington Step 2b: Determine transhorizon Bullington point

In the transhorizon case, the model must first determine the receiver horizon point using similar methods as those for the transmitter,

$$S_{rm} = \max_{i=2..(n-1)} \left[\frac{h_i - h_{rs} + 500 C_e d_i (d_p - d_i)}{d_p - d_i} \right],$$

and then calculate the distance of the Bullington point (see Figure 4) from the transmitter site, in kilometers, as

$$d_b = \frac{h_{rs} - h_{ts} + S_{rm} d_p}{S_{tm} + S_{rm}}.$$

With the location of the Bullington point known, the model can now evaluate the KED parameter associated with the effective knife-edge obstruction as

$$\nu_b = \left[h_{ts} + S_{tm} d_b - \frac{h_{ts}(d_p - d_b) + h_{rs} d_b}{d_p} \right] \left(\frac{0.002 d_p}{\lambda d_b (d_p - d_b)} \right)^{1/2}.$$

Finally, the algorithm determines an *uncorrected* diffraction loss $L_{uc} = J(\nu_b)$ in decibels using the approximate KED formula and proceeds to Step 3.

5.5 Bullington Step 3: Evaluate final diffraction losses

For either the LOS or transhorizon case, an empirical correction is necessary to arrive at our final Bullington diffraction loss for the entire path,

$$L_b = L_{uc} + (1 - \exp(-L_{uc}/6))\left(10 + 0.02 d_p\right),$$

expressed in decibels relative to direct transmission losses over the same path.

5.6 Example

I have run the Bullington method described above on a simple elevation profile where the average elevation is 10 m ASL with the exception of two obstructions at 4 and 6 km from the transmit point, as shown in the lower plot of Figure 5.

Figure 5. Example results for the Bullington method run on a simplified elevation profile with two obstacles. Upper plot (*red*) shows diffraction losses in decibels relative to direct transmission losses; lower plot (*blue*) shows the elevation profile itself.

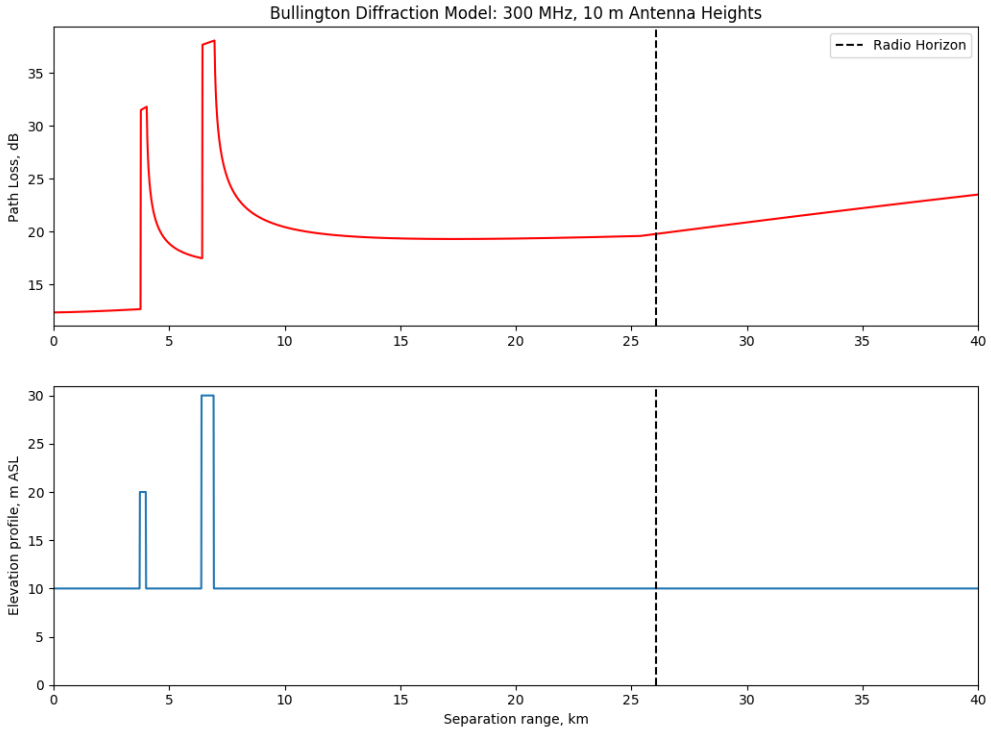

This example used $h_{tg} = h_{rg} = 10$ m AGL, and thus the radio horizon d_{LOS} occurs at roughly 26 km separation. Figure 5 shows that the method detects and accounts for both the shadow zones behind the two obstructions

and the interaction of the earth's bulge with the first Fresnel zone in the vicinity of the radio horizon. While qualitatively correct, the differences between the Bullington method results and experimental data (not to mention other, more rigorous models, such as Vogler 1982) are still significant, thus providing motivation for the development of the Delta-Bullington model described below and in ITU (2019).

6 Delta-Bullington Propagation Model

The Delta-Bullington model described in ITU Recommendation P.526-15 is an attempt to address some of the shortcomings of the Bullington model while maintaining computational simplicity and smoothly integrating direct transmission, spherical earth diffraction, and Bullington diffraction losses into a single coherent model (ITU 2019). A brief outline of the method is as follows, and I will use this numbering in subsequent subsections to aid in understanding.

1. Determine diffraction losses for the actual terrain path using Bullington's method. This loss is designated as L_{ba}, with the subscript denoting "Bullington" and "actual." However, as discussed in previous sections, it turns out that this loss estimate is not quite large enough.
2. Determine diffraction losses for the equivalent smooth-earth path using Bullington's method. This loss is stored in L_{bs}, with the subscript denoting "Bullington" and "smooth."
3. Determine diffractions losses over the spherical earth L_{sph} using methods discussed above in the "Smooth-Earth Diffraction" section.
4. The final loss reported by the Delta-Bullington method is $L_b = L_{ba} + \max(L_{sph} - L_{bs}, 0)$. If the spherical earth diffraction losses exceed those predicted by the Bullington method applied to a smooth earth, simply add the difference between them. If the path is truly smooth, then $L_{ba} = L_{bs}$ and the Bullington-derived losses cancel, leaving $L_b = L_{sph}$.

6.1 Delta-Bullington Step 1

Given the elevation profile of interest $d_{i=1..n}$ and $h_{i=1..n}$, apply the Bullington method to determine L_{ba}.

6.2 Delta-Bullington Step 2

To apply the Bullington method to an equivalent smooth-earth path, the algorithm must determine the effective transmit and receive antenna heights h'_{ts} and h'_{rs}, respectively, in m ASL relative to this path. The process for arriving at these values is fairly involved.

An equivalent smooth-earth path between transmitter and receiver can be defined using the two-point expression for a straight line,

$$h_{si} = \left(\frac{d_p - d_i}{d_p}\right) h_{st} + \left(\frac{d_i}{d_p}\right) h_{sr},$$

where the h_{si} are the n elevation points along the equivalent smooth-earth path, and $h_{st} = h_{s1}$ and $h_{sr} = h_{sn}$ are the heights (m ASL) of the smooth surface underneath the transmitting and receiving antennae, respectively. As h_{st} or h_{sr} are not known a priori, the algorithm requires two equations to solve for them, and these equations (for v_1 and v_2) are derived via least-squares fitting to the actual profile $d_{i=1..n}$ and $h_{i=1..n}$:

$$v_1 = \sum_{i=2}^{n} (d_i - d_{i-1})\,(h_i + h_{i-1})$$

$$v_2 = \sum_{i=2}^{n} (d_i - d_{i-1})\,[h_i(2d_i + d_{i-1}) + h_{i-1}(d_i + 2d_{i-1})]\,.$$

The smooth surface height (m ASL) under the transmitter is

$$h_{st} = \frac{2v_1 d_p - v_2}{d_p^2},$$

and the smooth surface height (m ASL) under the receiver is

$$h_{sr} = \frac{v_2 - v_1 d_p}{d_p^2}.$$

With the equivalent smooth-earth profile now defined, the algorithm searches for the highest obstruction height above this profile. The difference between actual and smooth profiles is

$$H_i = h_i - \frac{\left[h_{ts}(d_p - d_i) + h_{rs} d_i\right]}{d_p};$$

and, therefore, the highest obstruction above the smooth profile is

$$h_{obs} = \max_{i=1..(n-1)} (H_i).$$

The horizon elevation angle for the transmitter is evaluated as

$$\alpha_{obt} = \max_{i=1..(n-1)} (H_i/d_i)$$

while the horizon elevation angle for the receiver is

$$\alpha_{obr} = \max_{i=1..(n-1)} (H_i/(d_p - d_i)) .$$

These angles, both expressed in milliradians, are used to calculate provisional values for the ground elevation (m ASL) of the smooth surface at the transmitter and receiver ends of the path, h_{stp} and h_{srp}, respectively.

If $h_{obs} \leq 0$, then the highest obstruction is below the smooth profile and the original estimates based on least-squares fitting are used: $h_{stp} = h_{st}$ and $h_{srp} = h_{sr}$. Otherwise, the highest obstruction is above the smooth profile, and we must adjust our provisional values to

$$h_{stp} = h_{st} - h_{obs}\left(\frac{\alpha_{obt}}{\alpha_{obt} + \alpha_{obr}}\right)$$

$$h_{srp} = h_{sr} - h_{obs}\left(\frac{\alpha_{obr}}{\alpha_{obt} + \alpha_{obr}}\right).$$

For the final evaluation of the smooth surface heights below the transmitter and receiver, there are two cases to consider:

If $h_{stp} > h_1$ then $h_{std} = h_1$, otherwise $h_{std} = h_{stp}$.

If $h_{srp} > h_n$ then $h_{srd} = h_n$, otherwise $h_{srd} = h_{srp}$.

L_{bs} is determined by setting all $h_i = 0$ and running the Bullington model with effective transmit and receive antennae heights of $h'_{ts} = h_{ts} - h_{std}$ and $h'_{rs} = h_{rs} - h_{srd}$.

6.3 Delta-Bullington Step 3

Using the spherical earth diffraction model with path length d_p and with an effective transmitter antenna height of h'_{ts} and an effective receiver antenna height of h'_{rs}, evaluate L_{sph}.

6.4 Delta-Bullington Step 4

Determine the diffraction loss for the general path as

$$L_b = L_{ba} + \max(L_{sph} - L_{bs}, 0)$$

expressed in decibels over the direct transmission losses over the same path length d_p.

7 Tests of Delta-Bullington Method Implementation

7.1 ITU verification profiles

The ITU provides data to verify that a given implementation of the Delta-Bullington model is operating correctly. The verification data includes four different elevation profiles and a listing of both intermediate parameters and final diffraction losses for a variety of frequencies and antenna heights. In Figures 6 through 8, the elevation profile and the calculated total path loss (direct transmission and Delta-Bullington diffraction) for these paths are shown to demonstrate the general character of the predictions as a function of position over irregular terrain.

Figure 6. ITU Test Path 1 with $h_1 = h_2 = h_{ant} = 30$ m. The smooth-earth radio horizon is at the *dashed line*. This link includes losses associated with both obstacle and spherical earth diffraction. Note that these different loss phenomena are smoothly joined in the path loss curve.

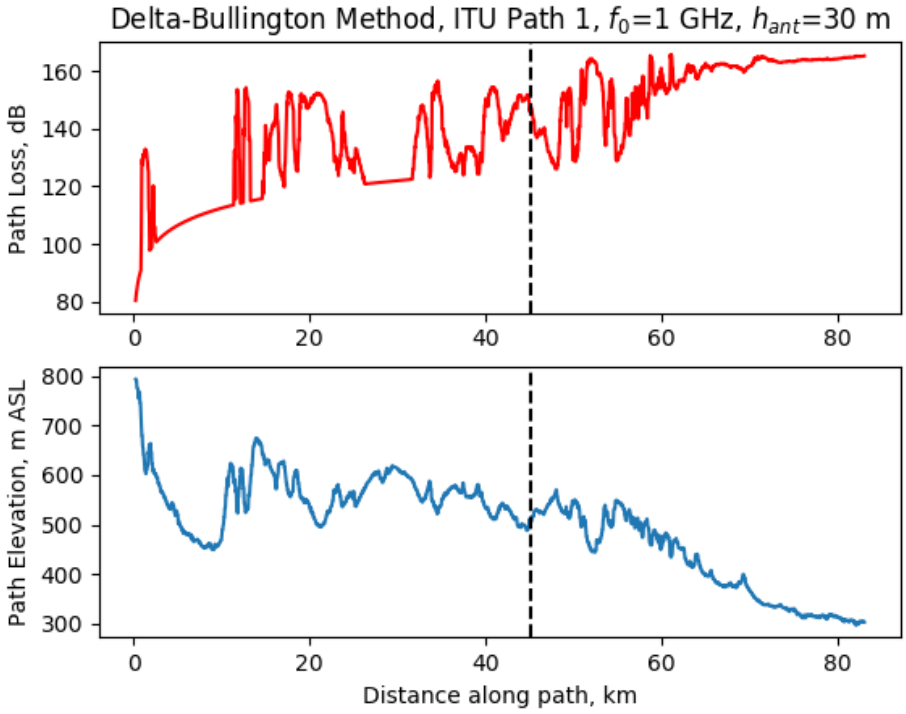

Figure 7. ITU Test Path 2 with $h_1 = h_2 = h_{ant} = 30$ m. The smooth-earth radio horizon is at the *dashed line*. This long link is transhorizon, involving losses due to obstacle and spherical earth diffraction.

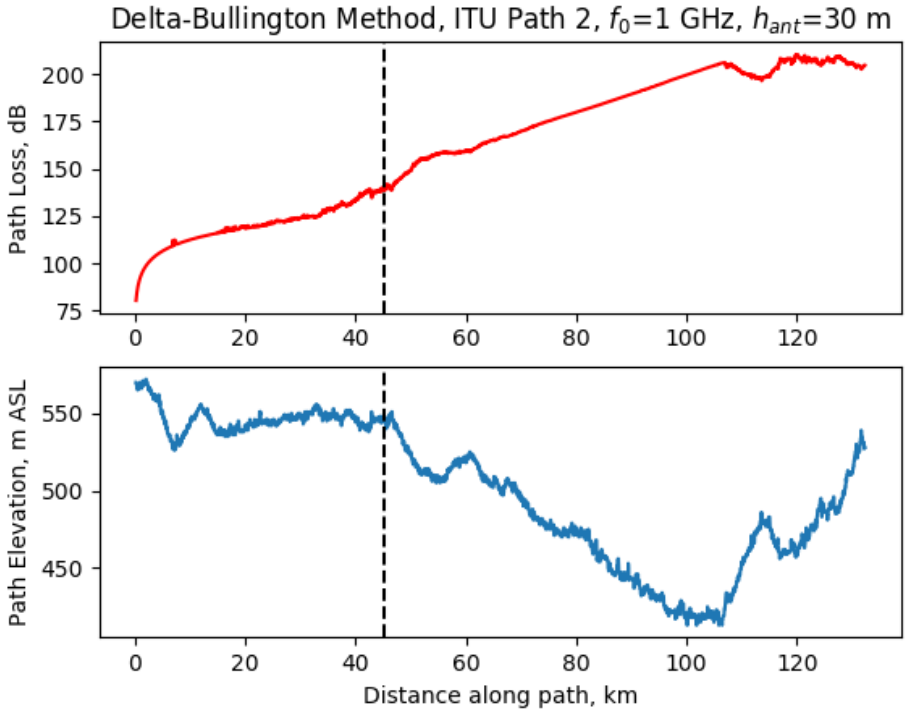

Figure 8. ITU Test Path 4 with $h_1 = h_2 = h_{ant} = 30$ m. Substantial losses occur even though this link is within the smooth-earth radio horizon, shown here as a *dashed line*.

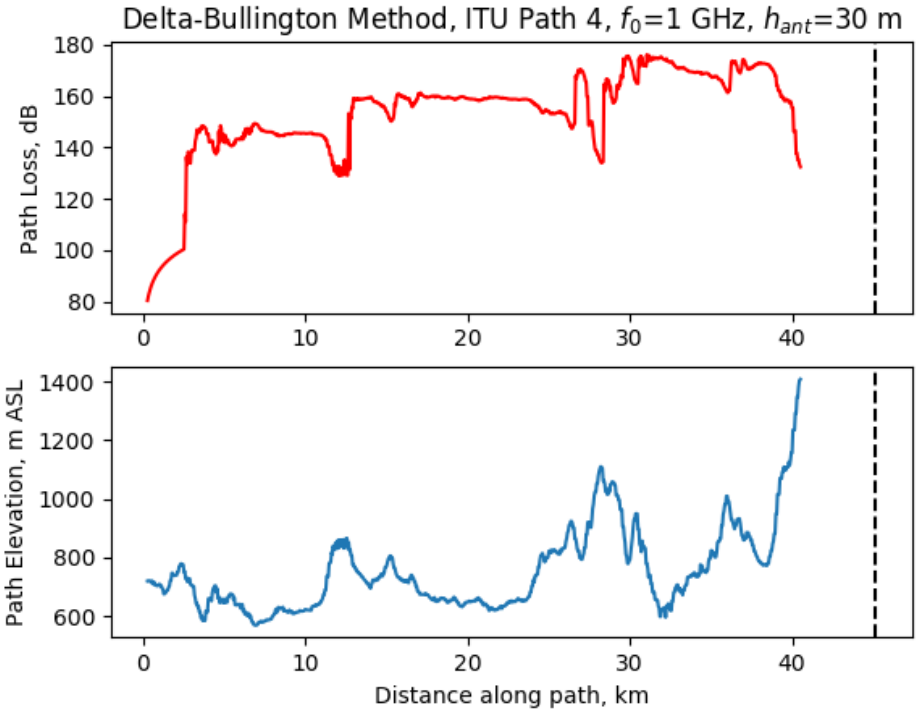

7.2 Reciprocity

An important test for any irregular terrain model is *reciprocity* (Durgin 2003). If the model respects reciprocity, then the predicted path losses from point A to point B will be the same (within a reasonable tolerance, such as 1 dB) as those predicted over the reverse path from point B to point A. I tested the reciprocal behavior of the Delta-Bullington model by running it on both the forward and reverse directions for ITU Test Paths 1, 2, and 4 and comparing the results as shown below in Table 1.

Table 1. Reciprocity testing results for the Delta-Bullington model (in decibels).

Elevation Profile	Direct Transmission Loss	Forward Diffraction Loss	Reverse Diffraction Loss	Forward-Reverse Difference
ITU Test Path 1	130.79	34.44	34.43	0.01
ITU Test Path 2	134.83	69.83	69.81	0.02
ITU Test Path 4	124.55	7.87	8.35	−0.48

The direct transmission losses shown in Table 1 are based on transmitter-receiver separation distance only and thus are the same in both forward and reverse directions. The small, predicted path loss differences between forward and reverse directions are negligible when compared with typical link budget uncertainties (one to several decibels) and variations associated with fading (several to 10 dB) encountered in practical radio links (Levis, Johnson, and Teixeira 2010).

7.3 Geographic and frequency continuity

A typical use case for this propagation loss model within EASEE is to determine the propagation losses at several frequencies over a wide spatial area surrounding a given transmitter or receiver. It is therefore critical that the Delta-Bullington model demonstrates continuity over the entire spectrum range and geographic area. To test the performance of this model, I have chosen a section of very rugged terrain in the White Mountains of New Hampshire as it is representative of both the environmental complexity and typical scale of tactical analyses needed by the Army.

The digital elevation model (DEM) used in these calculations was derived from the National Elevation Database, using 1/3 arc second elevation data, which was projected into Universal Transverse Mercator (UTM) coordinates. Elevation profiles were extracted from this DEM about a point centered on 44.2953° N, 71.2795° W (318149.2 m easting, 4907203.0 m

northing in UTM18 coordinates) for a full 360° of azimuth at 1° intervals and out to a range of 9 km using a uniform spatial sampling frequency equivalent to the 9 m resolution of the DEM. Antenna heights above ground level were fixed at 30 m for all analyses. The chosen 255 km² analysis region is especially rugged, containing the highest terrain relief within the state of New Hampshire.

Figure 9 shows the terrain, central analysis point, and 9 km radial extent of the analysis while Figure 10 shows polar plots of the propagation losses for 100 MHz and 1 GHz frequencies. Overall, the losses produced by the model are geospatially continuous over a wide range of terrain profiles, and the model predicts both LOS regions and deep shadow zones in locations consistent with the geometry of the central analysis point and the surrounding terrain. Because of the short range of the analysis and rugged nature of the chosen terrain for the test, changes in propagation losses with range associated with spherical earth diffraction losses are not expected, nor are they observed in the predictions.

Figure 9. Digital elevation model of the Presidential and Carter Ranges in New Hampshire in UTM coordinates. The center analysis point and 9 km radial extent of terrain used in subsequent propagation loss analyses are shown in *red*.

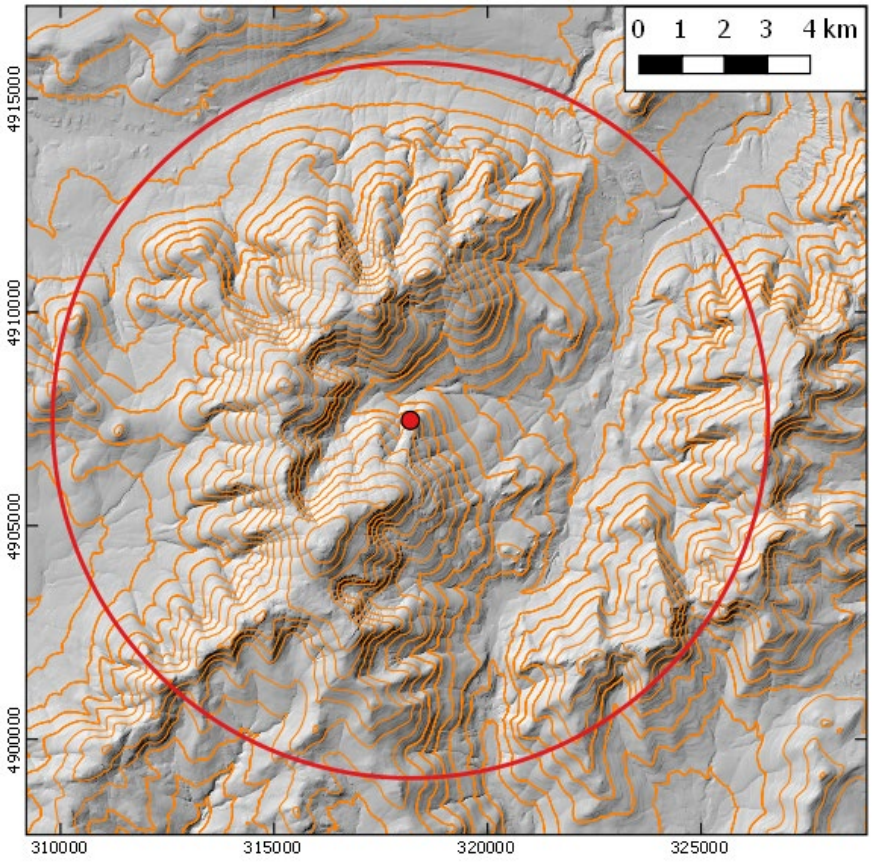

Figure 10. Delta-Bullington Model results for (*a*) 100 MHz and (*b*) 1000 MHz. Range rings are denoted in kilometers.

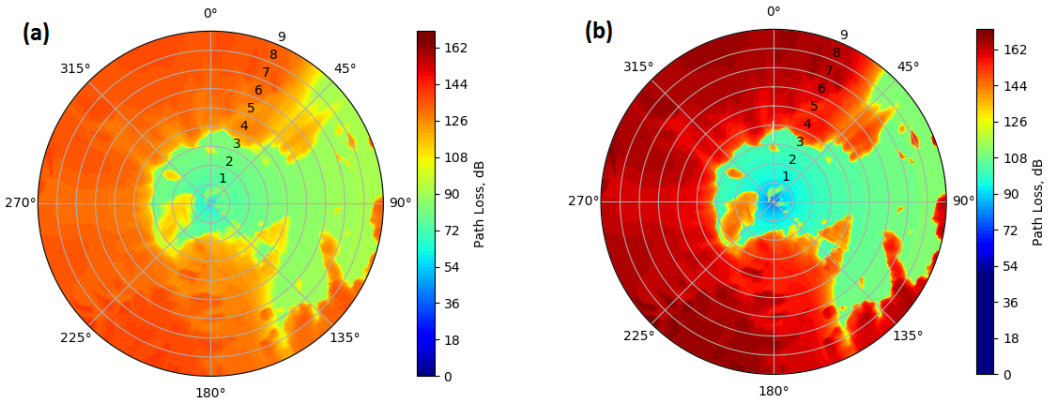

Increasing the RF of the analysis from 100 to 1000 MHz results in increased losses, both for the LOS and shadow zone cases. This is expected due to decreased effective isotropic antenna aperture and increased diffraction losses at higher frequencies (Levis, Johnson, and Teixeira 2010).

7.4 Model execution time and fidelity as a function of geographic resolution

The propagation loss modeling in the previous section was carried out at the maximum resolution of the underlying DEM and thus required considerable calculation time, over 13 minutes for each plot shown in Figure 10. Naturally, the computational time will vary with the type of processors used; but in general, computation times longer than a few minutes are unacceptable for the typical Army operational use case. As shown later in this section, analyses at such high resolutions are typically not necessary.

The comparison below was derived by timing the execution of the Delta-Bullington model operating on the same 255 km² area of mountainous terrain analyzed in the previous section and varying the number of elevation sampling points used to cover the area. In all cases, the elevation points were sampled at 360 azimuths, while the number of samples was set at 90, 250, 500, or 1000 samples along a given azimuth. All timing comparisons in this section were performed on a single Intel Core i7-3740QM CPU operating at 2.7 GHz.

Figure 11 shows that analysis time increases rapidly and nonlinearly with the number of analysis points used to cover the area. The nonlinear behavior with increasing analysis points is likely due to the increased density

of sampling points far from the central analysis point. Distant points require analysis of longer elevation profiles than those close in and therefore take more time. This behavior could potentially be overcome by carefully choosing the elevation profile points, exploiting the fact that the Delta-Bullington model does not require uniform spacing between profile points.

Figure 11. Single core execution time for the Delta-Bullington model applied to a 255 km² area at various resolutions.

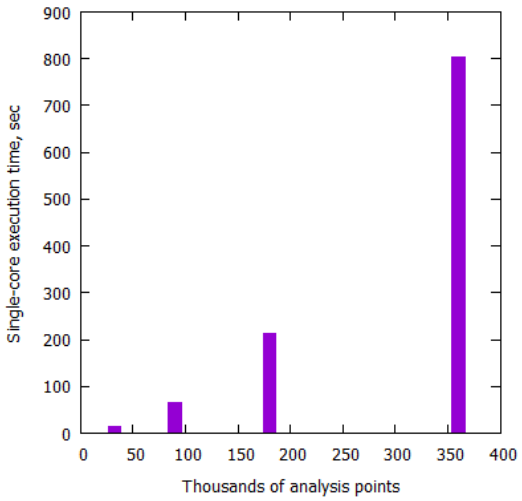

How significant are these changes in analysis resolution to the overall propagation loss prediction? Figure 12 plots the case with 1000 samples per azimuth line (~9 m intersample spacing) next to the case with 90 samples per azimuth (~100 m intersample spacing) and shows only a few subtle differences between the two predictions. The main differences are the magnitude of losses in very small shadow zones where the lower sampling rate perhaps missed the true maximum elevation point of the obstacle.

Figure 12. Comparison of Delta-Bullington propagation loss estimates for a frequency of 1000 MHz using elevation samples (*a*) every 9 m and (*b*) every 100 m along a given line of azimuth.

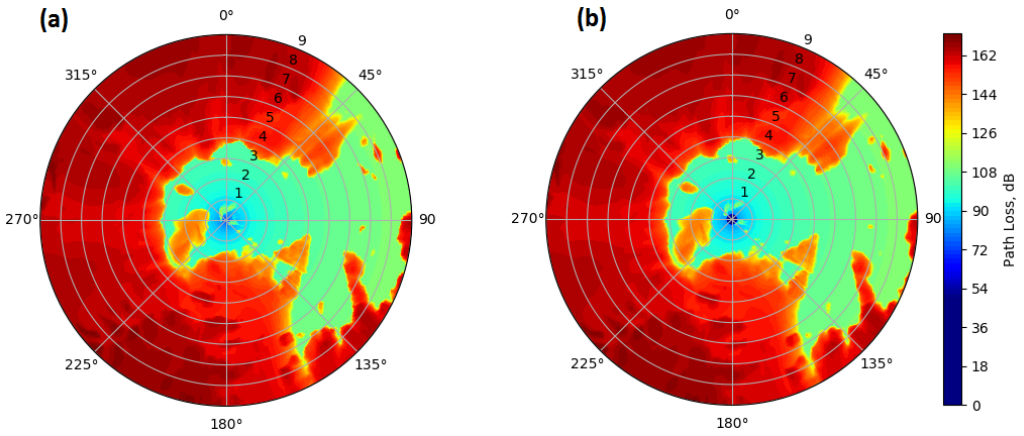

Overall, these estimates are quite similar both geographically, and in the magnitude of the propagation loss estimates. Based on this comparison, it is hard to justify the long calculation time of the high-resolution version compared against the 15 second calculation time of the low-resolution analysis.

8 Conclusion

I have described the main components of the Delta-Bullington model and how they interact to produce the continuous and believable path loss predictions over single and multiple geographically adjacent elevation profiles. This model has several advantages:

- Relatively straightforward implementation and input
- Does not require uniformly spatially sampled elevation profiles
- Smoothly joins terrain obstacle and smooth-earth diffraction losses
- Produces geographically continuous and topographically believable output in rugged terrain
- Reasonably rapid computational times over tactically relevant (few to tens of kilometers) ranges
- Respects reciprocity
- Is an international standard with documentation and verification data available

The main disadvantage of the Delta-Bullington model in the context of use within EASEE is that it is primarily designed for point-to-point analysis, with significant repetition of calculations when used at many points along a given elevation profile. The main use case for a RF propagation loss model within EASEE is analysis along many profiles, extracted as radial paths typically centered on a transmitter or receiver location within a DEM. It may be possible to optimize the model for analysis of an entire profile by storing some results from the previous calculation along the same radial, but this is beyond the scope of this project.

Overall, the Delta-Bullington model appears to be suitable for use within a decision-support tool like EASEE. If carefully implemented within EASEE, this model should enable rapid analysis of RF system performance in irregular terrain to support communications, surveillance, and sensor optimization planning.

References

Ayasli, S. 1986. "SEKE: A Computer Model for Low Altitude Radar Propagation over Irregular Terrain." *IEEE Transactions on Antennas and Propagation* (IEEE) 34 (8): 1013–1023. https://doi.org/10.1109/TAP.1986.1143933.

Bibb, D. A., J. Dang, Z. Yun, and M. F. Iskander. 2014. "Computational Accuracy and Speed of Some Knife-Edge Diffraction Models." In *Proceedings, 2041 IEEE Antennas and Propagation Society International Symposium (APSURSI),* 6–11 July, Memphis, TN, 705–706. https://doi.org/10.1109/APS.2014.6904683.

Bullington, K. 1947. "Radio Propagation at Frequencies above 30 Megacycles." *Proceedings of the IRE* (IEEE) 35 (10): 1122–1136. https://doi.org/10.1109/JRPROC.1947.232600.

Bullington, K. 1977. "Radio Propagation for Vehicular Communications." *IEEE Transactions on Vehicular Technology* (IEEE) 26 (4): 295–308. https://doi.org/10.1109/T-VT.1977.23698.

Deygout, J. 1966. "Multiple Knife-Edge Diffraction of Microwaves." *IEEE Transactions on Antennas and Propagation* 14 (4): 480–489. https://doi.org/10.1109/TAP.1966.1138719.

Durgin, G. D. 2008. "Practical Geometrical Behavior of Knife-Edge Diffraction." In *Proceedings, IEEE Antennas and Propagation Society International Symposium*, 5–11 July, San Diego, CA, 1–4. https://doi.org/10.1109/APS.2008.4619017.

Durgin, G. D. 2003. *Space-Time Wireless Channels*. Prentice Hall.

Egli, J. J. 1957. "Radio Propagation above 40 MC over Irregular Terrain." *Proceedings of the IRE* (IEEE) 45 (10): 1383–1391. https://doi.org/10.1109/JRPROC.1957.278224.

Eppink, D., and W. Kuebler. 1994. *TIREM/SEM Handbook*. ECAC-HDBK-93-076. Annapolis, MD: Electromagnetic Compatibility Analysis Center. https://apps.dtic.mil/dtic/tr/fulltext/u2/a296913.pdf.

Friis, H. T. 1946. "A Note on a Simple Transmission Formula." *Proceedings of the IRE* 34 (5): 254–256. https://doi.org/10.1109/JRPROC.1946.234568.

Giovaneli, C. L. 1984. "An Analysis of Simplified Solutions for Multiple Knife-Edge Diffraction." *IEEE Transactions on Antennas and Propagation* 32 (3): 297–301. https://doi.org/10.1109/TAP.1984.1143299.

Hufford, G. A., A. G. Longley, and W. A. Kissick. 1982. *A Guide to the Use of the ITS Irregular Terrain Model in the Area Prediction Mode*. NTIA Report 82-100. Boulder, CO: U.S. Department of Commerce, National Telecommunications and Information Administration. https://www.ntia.doc.gov/report/1982/guide-use-its-irregular-terrain-model-area-prediction-mode.

ITU (International Telecommunications Union). 2015. *Prediction Procedure for the Evaluation of Interference between Stations on the Surface of the Earth at Frequencies above about 0.1 GHz*. Recommendation P.452-16. Geneva: International Telecommunications Union. https://www.itu.int/rec/R-REC-P.452/en.

ITU (International Telecommunications Union). 2019. *Propagation by Diffraction*. Recommendation P.526-15. Geneva: International Telecommunications Union. https://www.itu.int/rec/R-REC-P.526-15-201910-I/en.

Kasampalis, S., P. I. Lazaridis, Z. D. Zaharis, A. Bizopoulos, L. Paunovska, S. Zettas, I. A. Glover, D. Drogoudis, and J. Cosmas. 2015. "Longley-Rice Model Prediction Inaccuracies in the UHF and VHF TV Bands In Mountainous Terrain." In Proceedings, *IEEE International Symposium on Broadband Multimedia Systems and Broadcasting*, 17–19 June, Chent, Belgium, 1–5. https://doi.org/10.1109/BMSB.2015.7177272.

Lebherz, M., W. Wiesbeck, and W. Krank. 1992. "A Versatile Wave Propagation Model for the VHF/UHF Range Considering Three-Dimensional Terrain." *IEEE Transactions on Antennas and Propagation* 40 (10): 1121–1131. https://doi.org/10.1109/8.182444.

Lee, W. C. Y. 1985. "Estimate of Local Average Power of a Mobile Radio Signal." *IEEE Transactions on Vehicular Technology* 34 (1): 22–27. https://doi.org/10.1109/T-VT.1985.24030.

Levis, C., J. Johnson, and F. Teixeira. 2010. *Radiowave Propagation: Physics and Applications*. Hoboken, NJ: John Wiley & Sons.

Lin, C. C., and J. P. Reilly. 1997. "A Site-Specific Model of Radar Terrain Backscatter and Shadowing." *Johns Hopkins APL Technical Digest* 18 (3): 432–447. https://www.jhuapl.edu/Content/techdigest/pdf/V18-N03/18-03-Lin.pdf.

Neskovic, A., N. Neskovic, and G. Paunovic. 2000. "Modern Approaches in Modeling of Mobile Radio Systems Propagation Environment." *IEEE Communications Surveys and Tutorials* 3 (3): 2–12. https://doi.org/10.1109/COMST.2000.5340727.

Okumura, Y., E. Ohmori, T. Kawano, and K. Fukuda. 1968. "Field Strength and Its Variability in VHF and UHF Land Mobile Service." *Review of the Electrical Communication Laboratory* 16 (9–10): 825–873.

Pogorzelski, R. J. 1982. "A Note on Some Common Diffraction Link Loss Models." *Radio Science* 17 (6): 1536–1540. https://doi.org/10.1029/RS017i006p01536.

Powell, J. R. 1983. *Terrain Integrated Rough Earth Model*. TN–83-002. Annapolis, MD: Electromagnetic Compatability Analysis Center.

Vogler, L. E. 1982. "An Attenuation Function for Multiple Knife-Edge Diffraction." *Radio Science* 17 (6): 1541–1546. https://doi.org/10.1029/RS017i006p01541.

Wilson, D. K., and K. K. Yamamoto. 2014. *Environmental Awareness for Sensor and Emitter Employment (EASEE): Software Design Version 2*. ERDC/CRREL TR-14-27. Hanover, NH: U.S. Army Engineer Research and Development Center, Cold Regions Research and Engineering Laboratory. http://hdl.handle.net/11681/5478.

Wilson, D. K., R. Bates, and K. K. Yamamoto. 2008. *Object-Oriented Software Model for Battlefield Signal Transmission and Sensing*. ERDC/CRREL TR-09-17. Hanover, NH: Engineer Research and Development Center, Cold Regions Research and Engineering Laboratory. http://hdl.handle.net/11681/5538.

Yamamoto, K. K., N. J. Reznicek, and D. K. Wilson. 2015. *Integration of Radio-Frequency Transmission and Radar in Multimodal Signal-Modeling Software*. ERDC/CRREL TR-15-12. Hanover, NH: U.S. Army Engineer Research and Development Center, Cold Regions Research and Engineering Laboratory. http://hdl.handle.net/11681/5339.

Yang, C.-F., W.-Y. Chang, W.-Y. Hwu, and H.-J. Li. 1998. "An Automated UTD Approach for Modeling Wave Propagation over Hilly Terrain Based on Digital Maps." In *Proceedings, IEEE Antennas and Propagation Society International Symposium*, 21–26 June, Atlanta, GA, 1880–1883. https://doi.org/10.1109/APS.1998.701570.

Acronyms and Abbreviations

CRREL	Cold Regions Research and Engineering Laboratory
DEM	Digital Elevation Model
EASEE	Environmental Awareness for Sensor and Emitter Employment
ERDC	U.S. Army Engineer Research and Development Center
ITM	Integrated Terrain Model
ITU	International Telecommunications Union
KED	Knife-Edge Diffraction
LOS	Line of Sight
m AGL	Meters above Ground Level
m ASL	Meters above Sea Level
RF	Radio Frequency
TIREM	Terrain Integrated Rough Earth Model
UTM	Universal Transverse Mercator

REPORT DOCUMENTATION PAGE

Form Approved
OMB No. 0704-0188

1. REPORT DATE (DD-MM-YYYY)	2. REPORT TYPE	3. DATES COVERED (From - To)
January 2022	Final Report	FY20–FY21

4. TITLE AND SUBTITLE
A Study on the Delta-Bullington Irregular Terrain Radiofrequency Propagation Model: Assessing Model Suitability for Use in Decision Support Tools

5a. CONTRACT NUMBER

5b. GRANT NUMBER

5c. PROGRAM ELEMENT

6. AUTHOR(S)
Daniel J. Breton

5d. PROJECT NUMBER

5e. TASK NUMBER

5f. WORK UNIT NUMBER

7. PERFORMING ORGANIZATION NAME(S) AND ADDRESS(ES)
U.S. Army Engineer Research and Development Center (ERDC)
Cold Regions Research and Engineering Laboratory (CRREL)
72 Lyme Road
Hanover, NH 03755-1290

8. PERFORMING ORGANIZATION REPORT NUMBER
ERDC/CRREL TR-22-1

9. SPONSORING / MONITORING AGENCY NAME(S) AND ADDRESS(ES)
U.S. Army Engineer Research and Development Center
3909 Halls Ferry Road
Vicksburg, MS 39180-6199

10. SPONSOR/MONITOR'S ACRONYM(S)

11. SPONSOR/MONITOR'S REPORT NUMBER(S)

12. DISTRIBUTION / AVAILABILITY STATEMENT
Approved for public release; distribution is unlimited.

13. SUPPLEMENTARY NOTES

Funded by the ERDC Future Innovation Fund, FAD/Customer Order 4902-XX-2460-08, "Terrain and Signature Physics Integration Center"

14. ABSTRACT

Modeling the propagation of radiofrequency signals over irregular terrain is both challenging and critically important in numerous Army applications. One application of particular importance is the performance and radio connectivity of sensors deployed in scenarios where the terrain and the environment significantly impact signal propagation. This report investigates both the performance of and the algorithms and assumptions underlying the Delta-Bullington irregular terrain radiofrequency propagation model discussed in International Telecommunications Union Recommendation P.526-15. The aim is to determine its suitability for use within sensor-planning decision support tools. After reviewing free-space, spherical earth diffraction, and terrain obstacle diffraction losses, the report discusses several important tests of the model, including reciprocity and geographic continuity of propagation loss over large areas of rugged terrain. Overall, the Delta-Bullington model performed well, providing reasonably rapid and geographically continuous propagation loss estimates with computational demands appropriate for operational use.

15. SUBJECT TERMS
Diffraction, Electromagnetics, Geospatial, Model assessment, Propagation, Radio, Radio wave propagation, Rural terrain, Signal processing

16. SECURITY CLASSIFICATION OF:			17. LIMITATION OF ABSTRACT	18. NUMBER OF PAGES	19a. NAME OF RESPONSIBLE PERSON
a. REPORT	b. ABSTRACT	c. THIS PAGE			19b. TELEPHONE NUMBER (include area code)
Unclassified	Unclassified	Unclassified	SAR	42	